

We are IntechOpen, the world's leading publisher of Open Access books Built by scientists, for scientists

4,800

Open access books available

122,000

International authors and editors

135M

Downloads

Our authors are among the

154

Countries delivered to

TOP 1%

most cited scientists

12.2%

Contributors from top 500 universities

**WEB OF SCIENCE™**Selection of our books indexed in the Book Citation Index
in Web of Science™ Core Collection (BKCI)

Interested in publishing with us?
Contact book.department@intechopen.com

Numbers displayed above are based on latest data collected.

For more information visit www.intechopen.com

Chapter

Solvent Effects on Dye Sensitizers Derived from Anthocyanidins for Applications in Photocatalysis

Diana Barraza-Jiménez, Azael Martínez-De la Cruz, Leticia Saucedo-Mendiola, Sandra Iliana Torres-Herrera, Adolfo Padilla Mendiola, Elva Marcela Coria Quiñones, Raúl Armando Olvera Corral, María Estela Frías-Zepeda and Manuel Alberto Flores-Hidalgo

Abstract

Anthocyanidins under the effects of solvents water, ethanol, n-hexane, and methanol are interesting due to their suitability as natural dyes for photocatalytic applications. In this chapter, DFT and TDDFT methodologies are used to study their electronic structure. The results displayed include HOMO, LUMO, HOMO-LUMO gap, chemical properties, and reorganization energies for the ground states, and excited state data are also displayed. Malvidin in gas phase has lower gap energy. After addition of solvents, gap energy increases in all cases but malvidin with n-hexane presents narrower gap. Conceptual DFT results show that cyanidin and malvidin may have good charge transfer. Cyanidin presented lower electron reorganization energy (λ_e) using solvent water; however, ethanol and methanol had similar values. TDDFT is used to calculate excited states, and absorption data show wavelength main peak between 479.1 and 536.4 nm. UV-Vis absorption spectra were generated and solvent effects on each molecule is discussed. Anthocyanidins work well in the visible region with the stronger peak at the green region. These pigments are good options for photocatalysis application and cyanidin and malvidin, in this order, may be the best choices for dye sensitization applications.

Keywords: anthocyanidins, dyes, solvent effects, DSSC, TDDFT

1. Introduction

Organic pigments have raised great interest in late years, may be driven by their potential in renewable energy applications which has been reinvigorated with the invention of dye-sensitized solar cells (DSSCs). Dye-sensitized solar cells (DSCs) are an attractive solar energy conversion technology and present advantages that include low cost of manufacture, ease of fabrication, and modifiable features such as color and transparency [1–5]. First DSSCs employed ruthenium (II)-based dyes in conjunction with iodide-based electrolytes to achieve an 11.9% solar-to-electric power conversion efficiency (PCE) [6]. A new generation of DSSCs based on naturally obtained

pigments is a great option as dye sensitizers, and this is the reason of a revitalized interest in these pigments [6, 12]. For example, porphyrin-based dyes have been tested as viable options, and they displayed great flexibility to work as panchromatic sensitizers [6, 13, 14]. It has been reported that porphyrin chromophore has strong light absorption around 400 nm in the blue region which is known as the Soret band or Soret peak and also in the Q-bands which is a region between slightly over 500 and 620 nm, but presents weak absorption in the region between these two features [6].

Then, it may be considered an interesting green option using organic pigments in DSSC technology. Analogously, these principles may be used to decompose chemical pollutants naturally without any contaminant waste. These organic pigments possess environmentally friendly properties, easy accessibility, and high absorption in the visible region which make them good candidates [7]. An alternative organic pigment to porphyrins may be anthocyanidins, a group of flavonoids contained in different parts of plants such as fruits, leaves, and flowers. Anthocyanidins may be considered water-soluble plant pigments that usually carry colors ranging from red to blue [8]. These natural pigments have shown health benefits and are commonly used colorants in food industry [9, 10].

Researchers continue to look for viable alternatives to ruthenium-based dyes and DSSC components in order to increase efficiency [11–15]. Natural pigments represent, in particular, a good option and among them anthocyanins are within our research interest [13–15]. These pigments have shown relevant advantages in DSSC technology, for example, they are metal-free, nontoxic, widely available, and inexpensive. They also have hydroxyl groups that benefit binding with TiO_2 and have been shown to be able to inject electrons into the TiO_2 conduction band at an ultrafast rate when excited with visible light [16]. There have been several studies on DSSC using anthocyanins as a photosensitizer with promising results [17–21]. The efficiency (η) from those studies, however, was generally quite low (0.5–0.6%). Recently, one of these reports [22] was carried out using sealed solar cells with enhanced electrodes (multilayer TiO_2 film plus a scattering layer), and anthocyanins contained organic acids demonstrated an efficiency of around 1.0%.

In nature, dyes can absorb visible light to enable plant photochemical processes; many of them are able to inject an electron into the conduction band of the semiconductor which is fundamental for photocatalytic processes [23]. This property is of great interest in dye-sensitized solar cells (DSSC), where dyes are used with a photocatalyst that may be a semiconductor oxide such as TiO_2 or ZnO for example [24]. An important consideration relates to prevent the degradation of the dye on a DSSC but this may not be the case for aqueous suspension of dye and photocatalyst. In such case, it may be confusing whether the dye degradation is due to dye sensitization itself or by action of the photocatalyst or under the influence of both factors [25, 26].

In regard to chemical processes, for chemical decoloration, the oxidation method is the most used because of its easy application. This method may be found in the literature as chemical oxidation and advanced oxidation process. Both these methods achieve the degradation of chemical dyes, pesticides among other pollutants, either partially or completely under ambient conditions [27]. The advanced oxidation process may be categorized in photocatalytic oxidation (use of light for activation of catalyst) and Fenton chemistry suitable for treating wastewater in particular for processes resistant to biological treatment [27].

Then, dye-sensitized process may be used in other applications and in this chapter, we will refer to its application in photocatalysis. This process uses light to activate a photocatalyst and represents a potential application to take advantage of sunlight for diverse processes such as gas purification, H_2 production, and water treatment. There are limitations for dye-sensitized semiconductors; for example,

in water purification, the organic dye may be diluted by water or at least erodes or deteriorates from the photocatalyst surface due to continuous interaction with water. Of course, the specific device configuration used during water treatment defines the disposition and interaction of the photocatalyst with the liquid and ultimately defines the severity of the fluid effects on the sensitizer layer. Dye sensitization effect may be a good choice for water treatment, but its effectiveness depends on the device disposition and the sensitizer presentation mainly when it gets in touch with the polluted water.

Among the different natural pigments, anthocyanidins represent an interesting alternative as dye sensitizing naturally obtained pigment. Since dye sensitizer and DSSC advances may be used in solar technology applications such as photocatalysis, this chapter presents interesting information related to anthocyanidins focused on its potential application in renewable energy applications and in particular when used as dye sensitizing pigment in photocatalysis. In particular, the chapter presents information related to an analysis of the effects caused by commonly used solvents to obtain anthocyanidins such as gas phase (as comparative basis), water, ethanol, n-hexane, and methanol and includes discussion on how several electronic properties of interest are subject to different effects in consequence depending on the selected solvent.

2. Anthocyanidin molecular structure

In this section, anthocyanidin structural data from published references and also our own results obtained with DFT methodology are presented. For convenience, structural data are presented in this section and computational details used in DFT calculations will be included in the next section.

2.1 Anthocyanidins structure

Anthocyanidins are natural pigments commonly found in plants with a molecular structure based on the flavylum ion or 2-phenylchromenylium (chromenylium may be referred to as benzopyrylium). These natural pigments are salt derivatives of the 2-phenylchromenylium cation, commonly known as flavylum cation. The more common anthocyanidins and their substitution pattern are shown in **Table 1**.

The phenyl group at the 2-position can carry different substituents that determine a particular anthocyanidin. With a positive charge, anthocyanidins differ from other flavonoids. Pigment molecule substituents and features are summarized in **Table 1** with a general interpretation of structural differences amongst variants, and a general scheme for anthocyanidins is displayed in **Figure 1**.

Name	Chemical formula	Substitution pattern		Color
		R1	R2	
Cyanidin	(C ₁₅ H ₁₁ O ₆) ⁺	OH	OH	Orange-red
Delphinidin	(C ₁₆ H ₁₁ O ₇) ⁺	OH	OH	Blue-red
Malvidin	(C ₁₅ H ₁₃ O ₅) ⁺	OCH ₃	OCH ₃	Blue-red
Pelargonidin	(C ₁₅ H ₁₁ O ₅) ⁺	H	H	Orange
Peonidin	(C ₁₅ H ₁₃ O ₆) ⁺	OCH ₃	H	Orange-red
Petunidin	(C ₁₅ H ₁₂ O ₆) ⁺	OCH ₃	OH	Blue-red

Table 1.
Six more common anthocyanidins with their variants.

The core of an anthocyanidin is a 15-carbon structure forming two aromatic rings (A and B in **Figure 1**) joined by a third ring (C) that contains an oxygen atom that provides the molecule positive charge. The presence of two C=C bonds in the C ring distinguishes anthocyanidins from other flavonoids and imparts a positive charge to the molecule, which results to be a cation (known as flavylium) in its stable form at low pH [28].

The phenylbenzopyrylium core of anthocyanins is typically modified by the addition of a wide range of chemical groups through hydroxylation, acylation, and methylation. In this section, structural data obtained with DFT geometry calculations are included as displayed in the next paragraphs.

2.2 Structure parameters for selected anthocyanidins using DFT

Structure calculations are needed in DFT methodology because every analysis by this methodology needs first of all relaxed geometries able to provide fundamental data for the molecules ground states. A ball-stick model was used to represent each of the constituent atoms (**Figure 2**).

To obtain molecular initial parameters, molecular database Chemical Entities of Biological Interest (ChEBI) [29] was consulted and three selected anthocyanidin molecules were downloaded from this database. Three of the more common anthocyanidin variants were selected for DFT calculations. These anthocyanidin models were used as initial input data for our DFT calculations. Within this section, our DFT results corresponding to geometry parameters for the selected three anthocyanidins, cyanidin, malvidin, and peonidin, respectively, are included. Bond length values, angles, and dihedral angles obtained from DFT calculations are shown in **Table 2**.

In general, C-C bond length found with the theoretical methodology used within this work is near to the typical value for the case of benzene; it is known that bonds have the same length of 140 pm. Benzene C-C bond length average value is between the generally known length of single and double C-C bonds of 154.0 and 134 pm, respectively. In average, for selected molecules, C-C bond length within this work is 139.9 pm.

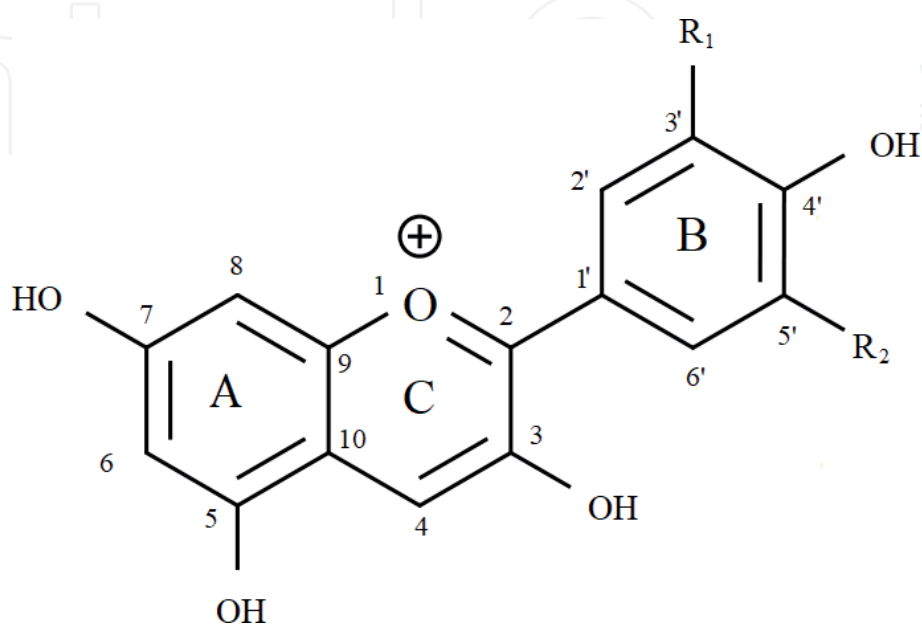


Figure 1.
Structure of anthocyanidins in their pristine form in correlation with **Table 1**.

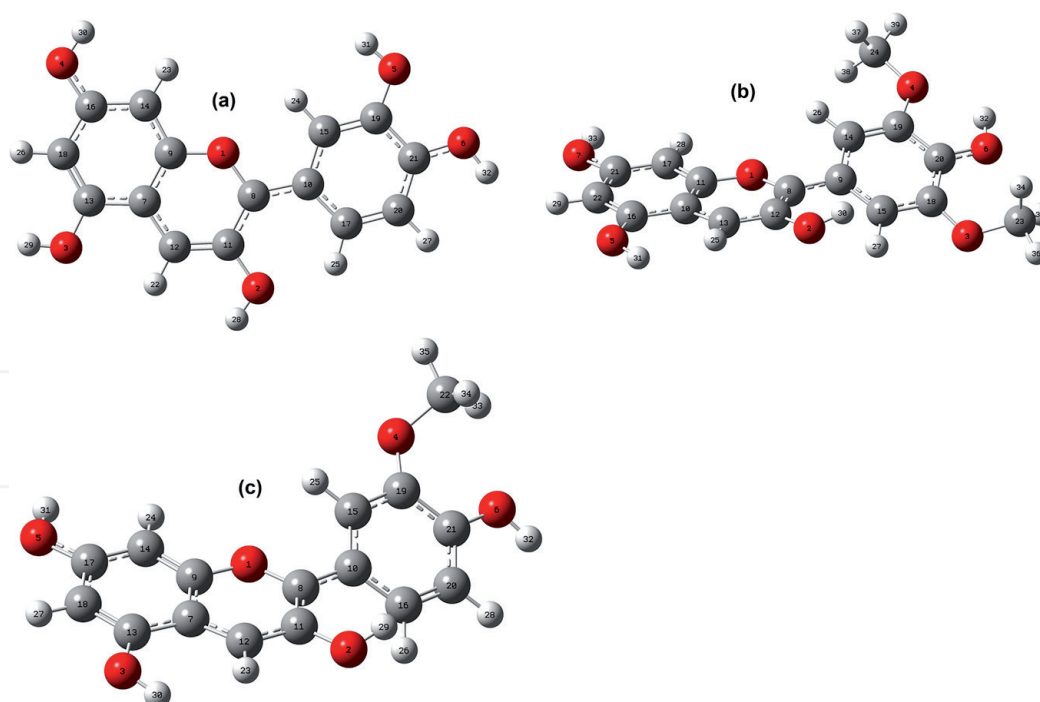


Figure 2. Selected anthocyanidin structure in their pristine form after geometry relaxation using DFT methodology, (a) cyanidin, (b) malvidin, and (c) peonidin.

Parameter	Cyanidin	Malvidin	Peonidin	Parameter	Cyanidin	Malvidin	Peonidin
O(1)-C(2)	1.350	1.347	1.345	C(3')-C(4')	1.422	1.418	1.420
O(1)-C(9)	1.358	1.359	1.358	C(4')-C(5')	1.396	1.407	1.399
C(2)-C(3)	1.420	1.407	1.404	C(5')-C(6')	1.383	1.395	1.384
C(2)-C(1')	1.436	1.444	1.447	O(1)-C(2)-C(1')-C(6')	180.0	151.4	150.1
C(3)-C(4)	1.382	1.388	1.390	C(3)-C(2)-C(1')-C(2')	180.0	149.3	149.1
C(4)-C(10)	1.403	1.399	1.397	O-C(3')-C(4')-C(5')	180.0	179.3	177.4
C(5)-C(6)	1.376	1.376	1.375	H-C(5')-C(4')-C(3')	180.0	175.9	178.5
C(5)-C(10)	1.427	1.435	1.436	O-C(4')-C(3')-C(2')	180.0	177.0	176.7
C(6)-C(7)	1.412	1.408	1.409	O-C(4')-C(5')-C(6')	180.0	178.0	177.7
C(7)-C(8)	1.395	1.398	1.398	C(8)-C(9)-C(10)-C(4)	180.0	176.3	175.9
C(8)-C(9)	1.386	1.382	1.381	O(1)-C(9)-C(10)-C(5)	180.0	178.8	178.7
C(9)-C(10)	1.409	1.421	1.423	C(8)-C(9)-O(1)-C(2)	180.0	179.9	179.4
C(1')-C(2')	1.422	1.414	1.409	C(5)-C(10)-C(4)-C(3)	180.0	179.3	179.5
C(1')-C(6')	1.414	1.407	1.411	C(9)-O(1)-C(2)-C(1')	180.0	179.1	179.0
C(2')-C(3')	1.377	1.381	1.387				

Table 2. Three selected anthocyanidins' geometric parameters, bond length, and bond angles in Å and °, respectively.

Our results for C-C bonds in average for selected anthocyanidins are within the range of 1.346–1.444 Å with <0.1 Å of difference between the larger and the shorter bonds for all cases. Literature reports for geometries include different methodologies such as B3LYP/6-31G(d) and B3LYP/6-31+G(d,p) [30–33]. All reports are in agreement that B3LYP reaches accurate results for this kind of molecules and overall C-C bond lengths are in good agreement with our results.

Dihedral angles are a good indication of the planarity in a structure; for anthocyanidins, we focused more in analyzing planarity among the three rings that form the molecule skeleton within each anthocyanidin. Also, the literature reports torsion angle as a parameter related to dihedral angles and this value may be used as a factor that helps differentiate anthocyanidins and their electronic structure behavior [30]. Dihedral values show that cyanidin is a planar molecule, selected values are 180°, and in general, all dihedrals are planar or differ with <1°. Peonidin presents more dihedrals that deviate from 180° but only a couple of dihedrals deviate by more than 5°. This last observation occurs for all the selected anthocyanidins; only a couple of dihedrals deviate in a significant amount from planarity but this small difference in the planarity determines the molecule character and its chemical properties. Then, only a few dihedrals indicate a nonplanar structure; these correspond to the relative angle variation observed in the B ring compared with the rest of the structure. These situations occur in all selected structures except in cyanidin which is a planar structure as shown by its dihedral values.

3. Solvents used to obtain anthocyanidins

In this section, literature related to the use of solvents during anthocyanidin extraction process is reviewed. Some differences in the material properties depending on the solvents used during its different chemical processes to obtain viable natural dye are expected. The same situation for anthocyanidins prevails, because different processes are used to obtain anthocyanidins in which it is needed to use different solvents resulting in behavior and property changes.

3.1 Anthocyanidin extraction

Anthocyanidin-rich extracts can be prepared from fresh, frozen, or dried plant materials. Examples of plants rich in anthocyanidins include blueberry [34], elderberry [35], and purple corn [36], among others. The particle size of source materials is an important factor during extraction; milling or grinding procedures among others are used with the goal of increasing surface area as well as the amount of compound obtained from the extraction process. Liquid nitrogen or lyophilization procedures may be complementary options during the grinding step to reduce anthocyanidin degradation. These are important recommendations given that the compounds involved may be subject to degradation caused by various factors, when carrying out the extraction procedure.

A general classification of extraction procedures is based in its phase used during the procedure such as solid or liquid extraction. Solid extraction is applied to liquid matrices, typically only during purification rather than extraction due to saturation of the absorbents. In the case of liquid extraction, a better recovery yield of anthocyanidins may be expected and for this reason, it is the more commonly used technique to extract these pigments from fruit sources. An important note captured from the literature is that there is a general practice that anthocyanidins are extracted with acidified water and polar organic solvents (methanol, ethanol,

and acetonitrile) due to their hydrophilic nature [37, 38]. More recently, other solvents have been used (e.g., lactic acid-glucose and choline chloride-malic acid mixtures) in an attempt to increase green alternatives to extract anthocyanidins to avoid toxic methodologies [37].

The extraction system can also require subsequent analytical procedures, which is an important consideration. For example, it is noticed that less polar solvents (such as ethanol and acetone) used for the extraction of anthocyanidins from haskap berries compressed the Sephadex LH-20 gel used for extract purification [38]. This step has been considered responsible for favorable results such as longer retention times when the fractions were analyzed by high-performance liquid chromatography and, additionally, the co-extraction of impurities. Less favorable notes that can be mentioned from this study relate to how acetone had a low extraction efficiency and formed anthocyanidin-derived complexes (5-methyl-pyranoanthocyanin) which were not found in fresh fruits [38].

In relation to the techniques, various methods have been developed to increase the efficiency of liquid extractions, decrease the processing time, and minimize the use and exposure to organic solvents. Examples are supercritical fluid extraction [39], pressurized liquid extraction [40], microwave-assisted extraction [41], and ultrasound-assisted extraction [42].

3.2 Solvents used to obtain anthocyanidins

Undoubtedly, solvents may be considered very important in the food, agro-chemical, chemical, and biotechnological, among others, process technologies. New streams of scientific research related to solvents are good alternatives for new experimentation. It may be worth mentioning the more relevant advances in this matter during the past two decades where supercritical fluids, ionic liquids, and deep eutectic solvents became the most outstanding subjects actively investigated as potential green solvents [43], in particular for the research associated with food, flavors, fragrances, and medicinal plants.

Another important perspective is solvents applied in industry, where the value of the products is not only dependent on the production costs themselves but also on the way of production. A critical aspect on the solvent selection for any process including industrial processes is related to safety. An aspect is avoiding the use of chemicals that are potentially dangerous for human health but extends also to have a solvent environmentally friendly including its disposal and also of the waste products containing the solvent. Nowadays, all these aspects need to be considered when real costs of production are calculated. For these reasons and the regulations, green technology is becoming an essential part of process cost and impact estimations. Above all, green technology is a critical aspect for solvent technology and starts as the first action to improve production processes including long and short-term impact [43] and relates directly on environmental matters and thus on earth survival.

4. DFT calculations, results, and discussion

In this section, DFT calculation results from our own research are displayed and analyzed. The first set of results contains ground state data, mainly related to energy results including molecular orbitals, energy gap, and relevant chemical properties. In the second set of results are included excited state data with their corresponding molecular orbital diagrams and absorption spectra based on TDDFT calculations.

4.1 Computational methods and details

All calculations were carried out in gas phase and using four different solvents, water, ethanol, n-hexane, and methanol. These solvents were selected because they are used commonly in the process to obtain pigments in the laboratory. PCM (polarizable continuum solvation model) was employed in the present work according to its implementation in G09 program suite. Anthocyanidin geometry was relaxed with B3LYP/6-311+g(d,p), and all of them were built resembling previously reported geometric parameters but a different theoretical method was used during the set of calculations.

Geometry optimizations and vibrational frequency analyses were carried out using DFT with the well-known B3LYP approach, which includes the interchange hybrid functional from Becke in combination with the correlation functional three parameter by Lee-Yang-Parr [44] 6-311+g(d,p) basis set as implemented in the Gaussian09 program package [45]. We selected 6-311+g(d,p) because after running a set of calculations with the selected natural pigments using the reported basis set for similar organic molecules, 6-311+g(d,p) result values were comparable to the different basis sets recommended by the literature. Furthermore, several research works reported that the B3LYP/6-311+g(d,p) theoretical method provides good results with a good level of accuracy for similar organic materials [46–50]. Each geometry optimization was followed by calculations for harmonic vibrational frequencies in order to confirm that a local minimum has been reached. After vibrational frequency results are obtained, the zero-point vibrational energy (ZPVE) and the thermal correction (TC) at 298.15 K were also included to complete these calculations. Energy calculations were performed for all molecules, adiabatic energies were obtained, and with these values, global and local chemical reactivity indexes were evaluated to find the electronic properties and some of its chemical properties such as HOMO, LUMO, gap, ionization potential (IP), electronic affinity (EA), electrophilicity (ω), electronegativity (χ), and hardness (η). All calculations were carried out in gas phase and using four different solvents, water, ethanol, n-hexane, and methanol. These solvents were selected because they are used commonly in the process to obtain pigments in the laboratory. PCM (polarizable continuum solvation model) was employed in the present work according to its implementation in G09 program suite.

Our results are compared with results by other research teams that worked with the selected molecules with other methodologies or experimentally and also the generally accepted TiO₂ was used as reference in its bulk presentation [46–50] to gain insight into the pigment application as dyes. Calculations were made for several excited states, but for practical purposes, only first excited states are displayed in the result table. Excited state calculations were carried out using TDDFT with the same theoretical method, B3LYP/6-311g+(d,p). Energy graphs and excited state spectral diagrams were developed using the Chemission code [51].

4.2 Electronic structure obtained from DFT calculations

Energy calculations for selected anthocyanidins were carried out with the B3LYP/6311+g(d,p) theoretical model for gas phase and using solvents water, ethanol, n-hexane, and methanol. To the best of our knowledge, this theoretical method has not been reported before for these specific molecules and solvents but other research groups have used other basis sets in their works. HOMO and LUMO molecular orbitals were calculated and these values are displayed in **Table 3**. The importance of molecular orbital calculation relies in the possibility that energy

orbitals in these pigments may overlap with a semiconductor energy orbital such as TiO₂ or ZnO for photocatalytic applications.

HOMO and LUMO are involved in the electronic transitions because the photo-induced electron transfers from the dye excited state to the semiconductor surface. It has been reported in the literature that dye sensitizer energy levels for HOMO and LUMO are required to match the potential of the electrolyte redox and the conduction band edge level of a semiconductor such as TiO₂ [46].

Selected anthocyanidins within this work at their ground and excited states match well with the redox level of the electrolyte (−4.85 eV) and the conduction band edge for TiO₂ (−4.00 eV) respectively, according to reported literature values [46–50].

Molecular orbitals were calculated for selected anthocyanidins in gas phase and using solvents water, ethanol, n-hexane, and methanol. LUMO values for anthocyanidins are between −6.856 and −6.624 eV for gas phase LUMO molecular orbital may be the more important contribution from these pigments if used as dye sensitizers. Anthocyanidin LUMO contribution may enable molecular orbital to overlap semiconductor band gap with dye conduction band, and so, it can enable an easier charge transfer process in DSSC applications.

For molecules with solvents water, ethanol, and methanol caused similar effect in the molecular orbitals' energy and because of these solvents' value shift in around 3 eV. These three solvents had a similar effect in HOMO molecular orbital with similar shift magnitude around 3 eV. Then n-hexane causes a smaller shift in molecular orbitals with <1.5 eV in both HOMO and LUMO. HOMO and LUMO molecular orbitals and additional energy levels are displayed in **Figures 3** and **4**.

HOMO-LUMO energy difference is a good approximation to the material's band gap. For the selected anthocyanidins, energy gap was between 2.539 and 2.881 eV in gas phase with malvidin having the narrower gap.

Pigment	Solvent	H-L	HOMO	LUMO	λ_e	EEP	λ_{it}	HEP
(C ₁₅ H ₁₁ O ₆) ⁺	Gas phase	2.664	−9.288	−6.624	0.318	5.525	0.344	10.361
	Water	2.824	−6.452	−3.628	0.262	4.064	0.284	6.038
	Ethanol	2.816	−6.528	−3.712	0.264	4.102	0.288	6.155
	n-hexane	2.712	−7.916	−5.204	0.295	4.818	0.324	8.284
	Methanol	2.818	−6.501	−3.683	0.263	4.089	0.267	6.115
(C ₁₅ H ₁₃ O ₅) ⁺	Gas phase	2.539	−9.24	−6.701	0.371	5.666	0.452	10.162
	Water	2.823	−6.532	−3.709	0.294	4.172	0.46	5.946
	Ethanol	2.81	−6.61	−3.8	0.295	4.216	0.462	6.066
	n-hexane	2.657	−7.975	−5.318	0.335	4.968	0.479	8.169
	Methanol	2.815	−6.583	−3.768	0.294	4.201	0.461	6.024
(C ₁₅ H ₁₃ O ₆) ⁺	Gas phase	2.691	−9.465	−6.774	0.364	5.703	0.498	10.371
	Water	2.955	−6.668	−3.713	0.293	4.173	0.527	6.019
	Ethanol	2.945	−6.748	−3.803	0.294	4.217	0.527	6.142
	n-hexane	2.815	−8.166	−5.351	0.328	4.98	0.533	8.316
	Methanol	2.948	−6.72	−3.772	0.294	4.202	0.527	6.100

H-L is HOMO-LUMO gap energy band. All units are in eV.

Table 3.
 Selected anthocyanidins' energy results using DFT (B₃LYP/6311+g(d,p)) in gas phase and with different solvents.

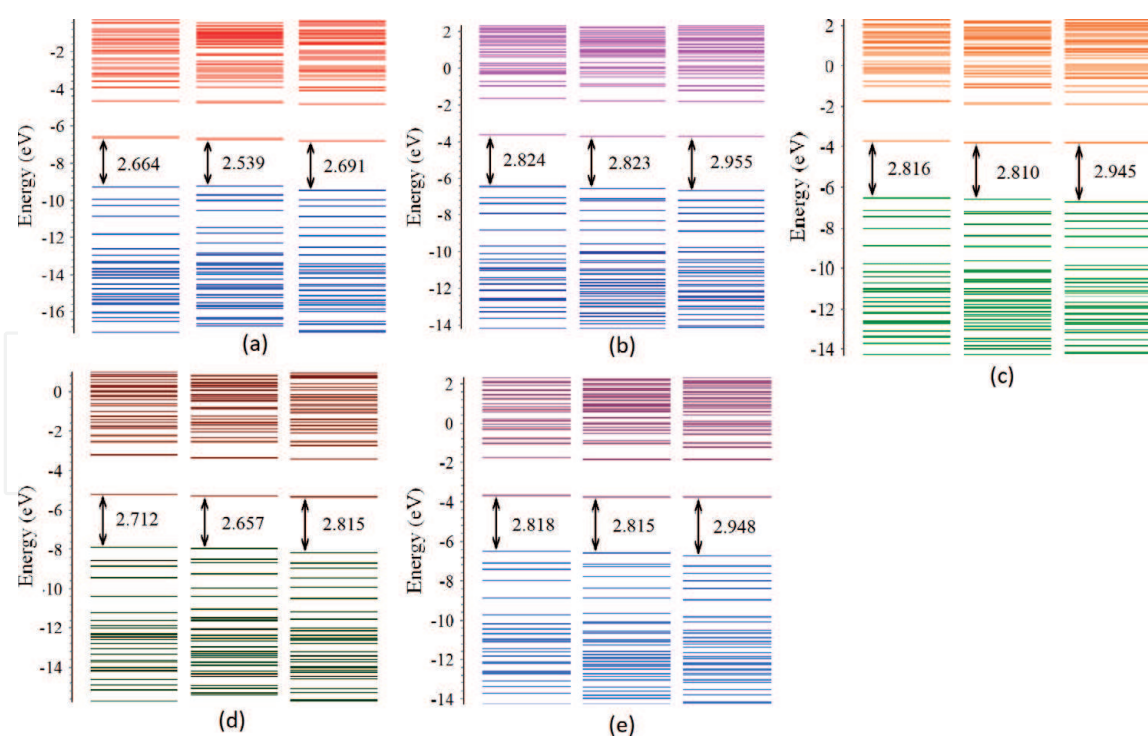


Figure 3. Molecular orbitals for selected anthocyanidins cyanidin, malvidin, and peonidin corresponding to (a) gas phase, (b) water, (c) ethanol, (d) *n*-hexane, and (e) methanol. H-L gap energy units are shown in eV.

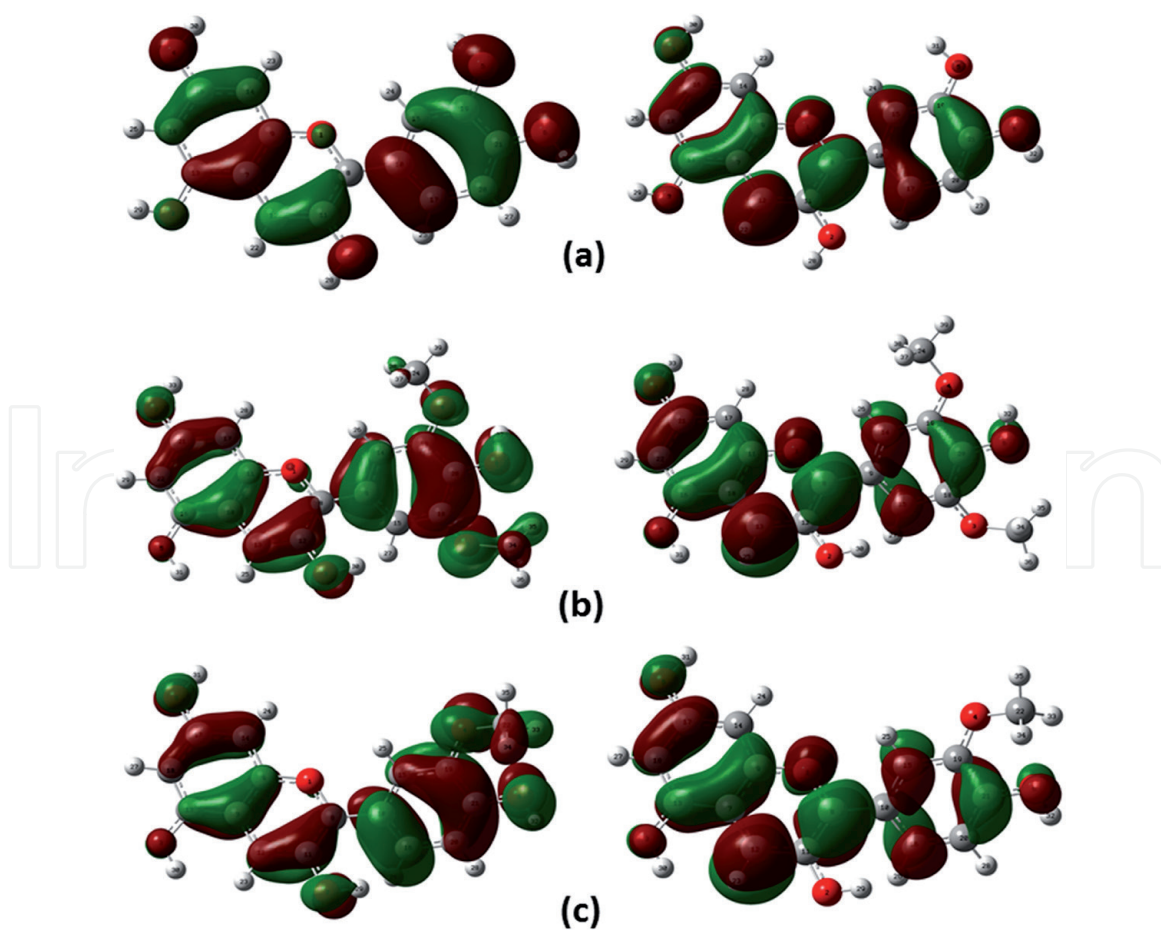


Figure 4. HOMO and LUMO molecular orbital charge distributions using $B_3LYP/6-311 + g(d,p)$, corresponding to: (a) cyanidin, (b) malvidin, and (c) peonidin.

When solvents either water, ethanol, n-hexane, or methanol are added, H-L values shift slightly for all selected pigments. Malvidin in its gas phase has a lower value for gap energy, and with addition of solvents, H-L increases in all cases but malvidin with n-hexane is the narrower. Solvent addition has a more noticeable effect for water solvent if compared with ethanol and methanol.

Overall, H-L values are similar in magnitude for all selected pigments when using either solvent water, ethanol, n-hexane, or methanol. The H-L shift in all cases is <10% if compared with their H-L values for its respective gas phase. Malvidin and peonidin presented the bigger shift with 11 and 10%, respectively, with the exception of malvidin using n-hexane which had a shift of 5%. Among selected solvents, water caused the bigger H-L shift and n-hexane caused the smaller shift. Energy gap of anthocyanidins has few variations with ~0.3 eV as the mean difference between variants. Overall, planarity and the relative angle among rings have small contribution to gap energy results and predominates their family common features to determine the H-L parameter.

Intramolecular reorganization energies were calculated to find the required energy for the molecule to go from neutral to ionized state (as cation if charge is lost and anion if charge is accepted). Also, these calculations help understand the inverse process when the ionized molecule becomes neutral and these two different processes relate to the charge transfer process.

Values as low as possible are desirable for reorganization energies so the available energy is used in the charge transfer process instead of using the energy in reorganization processes in such a way that λ should be as low as possible in order to avoid wasting solar energy instead of taking advantage of sunlight during the energy transferring process. Overall, solvent addition helps the pigment decrease λ , and display similar values for water, ethanol, and methanol. Solvent n-hexane also helps decrease λ values but with less impact than the other solvents. From selected anthocyanidins, cyanidin presented lower electron reorganization energy (λ_e) using solvent water but ethanol and methanol had similar values.

For the hole reorganization energy (λ_h), again cyanidin had the lower values but now with methanol solvent followed by water and methanol with near values but not as close as for λ_h . Hole extraction potential (HEP) and the electron extraction potential (EEP) were calculated, and the results overall present the higher values for gas phase and the value for each case is decreased when any of the selected solvents are added.

When n-hexane solvent decreases around 8 eV and with water, ethanol, and methanol as solvents HEP is around 6 eV. For EEP, a similar effect occurs but the values decrease in less than around 1 eV when water, ethanol, and methanol solvents are used and around 0.5 eV when n-hexane is used. The three variant anthocyanidins had similar values in gas phase with <0.1 eV of difference.

Reorganization energies show that malvidin is the best choice for sensitization applications. Electron energy λ_e indicates clearly that cyanidin with methanol is the best choice followed by water and ethanol.

For hole energy λ_h also cyanidin with the same solvents is the best choice; this behavior with λ values may be attributed to its molecular planarity. EEP and HEP are not as clear as λ ; in the case of these two parameters, malvidin with solvent water is the best choice but only with slight differences for the same solvent in other molecules like cyanidin and peonidin.

4.3 Chemical properties calculated from DFT results

Conceptual DFT was used to calculate the chemical properties of these three selected anthocyanidin variants. Chemical property results are shown in **Table 4**.

Pigment	Solvent	IP	EA	χ	η	ω	S
(C ₁₅ H ₁₁ O ₆) ⁺	Gas phase	10.642	5.154	7.898	2.744	11.439	0.364
	Water	6.322	3.802	5.062	1.26	10.165	0.793
	Ethanol	6.443	3.838	5.141	1.302	10.147	0.768
	n-Hexane	8.608	4.522	6.565	2.043	10.549	0.49
	Methanol	6.382	3.825	5.104	1.278	10.189	0.782
(C ₁₅ H ₁₃ O ₅) ⁺	Gas phase	10.614	5.296	7.955	2.659	11.899	0.376
	Water	6.406	3.878	5.142	1.264	10.462	0.791
	Ethanol	6.528	3.921	5.224	1.304	10.469	0.767
	n-Hexane	8.647	4.633	6.64	2.007	10.983	0.498
	Methanol	6.486	3.906	5.196	1.29	10.466	0.775
(C ₁₅ H ₁₃ O ₆) ⁺	Gas phase	10.869	5.34	8.105	2.765	11.879	0.362
	Water	6.545	3.881	5.213	1.332	10.199	0.751
	Ethanol	6.67	3.922	5.296	1.374	10.209	0.728
	n-Hexane	8.85	4.652	6.751	2.099	10.859	0.477
	Methanol	6.627	3.908	5.267	1.359	10.205	0.736

Values include ionization potential (IP), electron affinity (EA), electronegativity (χ), chemical hardness (η), electrophilicity index (ω), and chemical softness (S), all of them in eV.

Table 4.
Chemical property results for selected anthocyanidins.

Ionization potential (IP) is the needed energy to extract an electron from a neutral molecule in order to form a cation. This property is related with the stiffness of the electronic cloud. In regard to reactivity, the cloud is more reluctant to participate in electron transfer. Then, a lower ionization potential value is desirable so there is a higher molecular potential to serve as an electron donor. The molecule with the lower IP was malvidin in its gas phase but with solvent addition, IP decreased in all cases. Although water, ethanol, and methanol cause a similar effect in IP magnitude, it was water used as solvent in cyanidin, the variant with the lower IP value among all variants. IP in gas phase was around 11 eV for selected anthocyanidins and when water, ethanol, and methanol were used, IP decreased to values around 6 eV.

Solvent n-hexane also had a decreasing effect in IP values but the values were observed around 8 eV. Cyanidin using water and methanol presented lower IP values and other molecules like malvidin also presented their lower values with water and methanol.

Selected anthocyanidins in gas phase had EA values around 5 eV and with solvents water, ethanol, and methanol, values decreased to around 3 eV while n-hexane effect decreased the EA to around 4 eV. Regarding electronegativity (χ), it is calculated to estimate the capacity of molecules to attract electron pairs. The highest the χ value, the highest its suitability to act as a charge acceptor.

In general, selected anthocyanidins had χ values around 8 eV, and with solvents like water, ethanol, and methanol this value decreased to around 5 eV while n-hexane solvent effect was less with values around 6 eV.

Overall, the chemical properties estimated display some similarity among calculated values which may be attributed to molecular resemblance such as relative angle at ring B, and the differentiator relates to the small structural differences as well as their molecule constituents.

4.4 Excited states for absorption energy calculation using TDDFT

Excited states were calculated using the TDDFT scheme as implemented in Gaussian09 using the B3LYP/6311+g(d,p) theoretical method for selected anthocyanidins. B3LYP has been reported as an efficient hybrid functional that has been compared with several other functionals with good results [46–50, 52] to process different anthocyanins and anthocyanidins. For any DSSC to be effective, its absorption spectrum must match the solar irradiation spectrum. The absorption property of the dye determines its light harvesting capability and thus affects the performance of dye sensitizers in DSSCs [53–57].

Our calculations showed that there is a slight difference with experimental values due to solvent effects and variation contributed by measuring methodologies [52, 58–60]. Two main regions in the anthocyanidin UV-Vis spectra have been reported in the literature, the first located between 260 and 280 nm and the second is located at the visible region between 490 and 550 nm. A third peak appears at 310–360 nm [59]; our discussion will focus on the principal peak located in the visible region.

Molecule	Solvent	State	ΔE (eV)	λ (nm)	Transition	Contribution	f
$(C_{15}H_{11}O_6)^+$	Gas phase	1	2.546	487.1 (522*)	H \rightarrow L	67%	0.507
					H-1 \rightarrow L	17%	
	Water	1	2.524	491.2	H \rightarrow L	68%	0.619
					H-2 \rightarrow L	12%	
	Ethanol	1	2.528	490.4	H \rightarrow L	68%	0.629
					H-1 \rightarrow L	15%	
	n-Hexane	1	2.473	501.4	H \rightarrow L	69%	0.686
					H-2 \rightarrow L	12%	
	Methanol	1	2.524	491.3	H \rightarrow L	68%	0.622
					H-1 \rightarrow L	17%	
					H-2 \rightarrow L	12%	
	$(C_{15}H_{13}O_5)^+$	Gas phase	1	2.312	536.4 (542*)	H \rightarrow L	60%
Water		1	2.434	509.3	H-1 \rightarrow L	30%	0.604
Ethanol		1	2.481	499.8	H \rightarrow L	68%	0.591
					H-2 \rightarrow L	17%	
n-Hexane		1	2.376	521.9	H \rightarrow L	70%	0.627
Methanol		1	2.431	510.1	H \rightarrow L	61%	0.601
$(C_{15}H_{13}O_6)^+$	Gas phase	1	2.401	516.3 (532*)	H \rightarrow L	67%	0.288
					H-1 \rightarrow L	11%	
	Water	1	2.509	494.2	H \rightarrow L	69%	0.53
	Ethanol	1	2.564	483.6	H \rightarrow L	67%	0.515
	n-Hexane	1	2.465	503	H \rightarrow L	69%	0.535
	Methanol	1	2.505	494.9	H \rightarrow L	69%	0.527

Table 5.
 Excited state absorption results for selected anthocyanidins using TD-DFT.

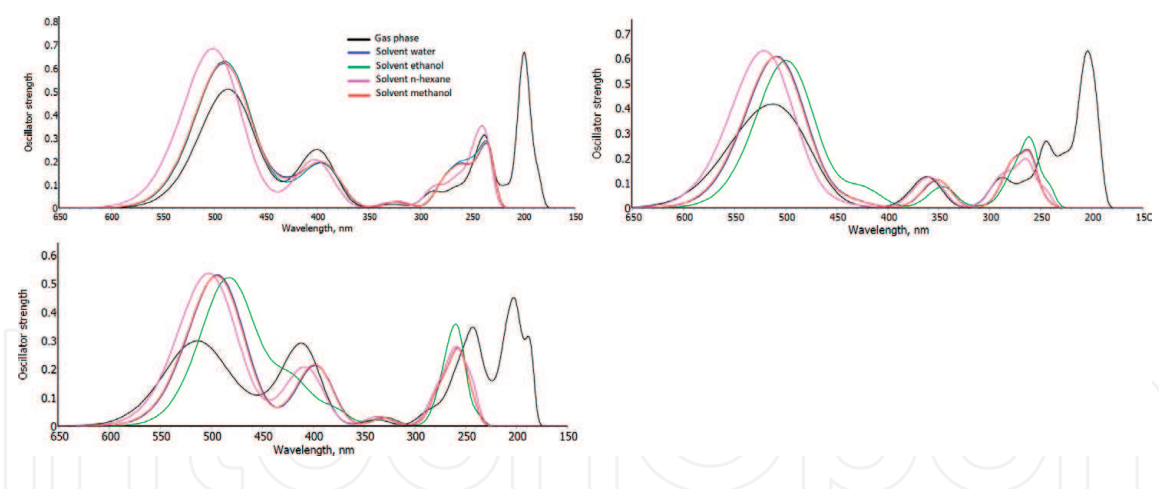


Figure 5. Anthocyanidin excited state spectra from results using the TD-DFT scheme for gas phase and solvents water, ethane, n-hexane, and methane corresponding to: (a) cyanidin, (b) malvidin, and (c) peonidin.

In a general view of absorption results, selected anthocyanidins in gas phase had absorption wavelength between 479.1 and 536.4 nm so, all selected molecules work in the visible part of the electromagnetic spectrum. Cyanidin works in the blue region and displays lower values calculated for wavelength. Malvidin has higher values while cyanidin presents a similar value. These results suggest that there is an effect caused by the small relative angle at B ring considering that these molecules are the simplest regarding their constituents. Addition of solvent shifts the absorption spectrum by increasing its wavelength by <5 nm in the case of water, ethanol, and methanol. For n-hexane solvent, absorption spectrum shifts the wavelength by slightly more than 10 nm.

First excited state values using TDDFT to calculate absorption data are displayed in **Table 5** and absorption spectrum is shown in **Figure 5**. The visible and near-UV regions are the most important for photon-to-current conversion to obtain the microscopic information about the electronic transitions and their corresponding MO properties.

5. Conclusions

Ground state geometries were analyzed using a well-known theoretical methodology, and an analysis on their relative angles comparing dihedrals within individual rings provides insight into the different planarity characteristics between rings and establishes that functionalization with OCH_3 is an important feature for the structural and energy gap differences. Molecular orbitals are analyzed and compared with our results from prior research for TiO_2 , the more widely used photocatalyst. These results mainly with MO analysis show that there is good compatibility between the semiconducting oxide and these pigments if they are to be used as dye sensitizers. Malvidin in its gas phase has a lower value for gap energy and with addition of solvents, gap energy increases in all cases but malvidin with n-hexane is the narrower. Conceptual DFT results show that cyanidin and malvidin may have good charge transfer. Furthermore, excited state data display the absorption capabilities of the selected pigments and confirm that cyanidin and malvidin, in that order, may be the best choices for dye sensitization applications.

Acknowledgements

This work was financed by CONACyT (Mexican Science and Technology National Council) through 2015 CONACyT SEP-CB (Basic Science-Public

Education Ministry) project fund 258553/CONACyT/CB-2015-01. MAFH thanks CONACyT for a postdoctoral scholarship (2014). Thanks to the Scientific Computational Laboratory at FCQ-UJED for computational resources. Thanks to Academic Group UJED-CA-129 for valuable discussions.

Conflict of interest

Authors state that this research was completed without any conflicts of interest related with funding to develop the present work.

Author details

Diana Barraza-Jiménez¹, Azael Martínez-De la Cruz², Leticia Saucedo-Mendiola¹, Sandra Iliana Torres-Herrera³, Adolfo Padilla Mendiola¹, Elva Marcela Coria Quiñones^{1,4}, Raúl Armando Olvera Corral¹, María Estela Frías-Zepeda^{1,5} and Manuel Alberto Flores-Hidalgo^{1*}

¹ Department of Chemical Sciences, Juarez University of Durango State, Durango, México

² Graduate Studies Division, Faculty of Mechanical and Electrical Engineering, Autonomous University of Nuevo Leon, San Nicolás de los Garza, NL, Mexico


³ Faculty of Forestry Science, Juarez University of Durango State, Durango, México

⁴ TecNM/Durango Institute of Technology, Durango, Mexico

⁵ CIIDIR-IPN, Durango, México

*Address all correspondence to: maflores.hidalgo02@gmail.com

IntechOpen

© 2019 The Author(s). Licensee IntechOpen. This chapter is distributed under the terms of the Creative Commons Attribution License (<http://creativecommons.org/licenses/by/3.0>), which permits unrestricted use, distribution, and reproduction in any medium, provided the original work is properly cited. 

References

- [1] Mathew S, Yella A, Gao P, Humphry-Baker R, Curchod BFE, Ashari-Astani N, et al. Dye-sensitized solar cells with 13% efficiency achieved through the molecular engineering of porphyrin sensitizers. *Nature Chemistry*. 2014;**6**:242-247
- [2] O'Regan B, Grätzel M. A low-cost, high-efficiency solar cell based on dye-sensitized colloidal TiO₂ films. *Nature*. 1991;**353**:737-740
- [3] Grätzel M. Conversion of sunlight to electric power by nanocrystalline dye-sensitized solar cells. *Journal of Photochemistry and Photobiology A*. 2004;**164**:3-14
- [4] Grätzel M. Dye-sensitized solar cells. *Journal of Photochemistry and Photobiology C*. 2003;**4**:145-153
- [5] Komiya R et al. Improvement of the conversion efficiency of a monolithic type 8 dye-sensitized solar cell module. In: *Technical Digest, 21st International Photovoltaic Science and Engineering Conference 2 C-50-08*. 2011
- [6] Yella A et al. Porphyrin-sensitized solar cells with cobalt (II/III)-based redox electrolyte exceed 12 percent efficiency. *Science*. 2011;**334**:629-634
- [7] Shrestha M et al. Dual functionality of BODIPY chromophore in porphyrin-sensitized nanocrystalline solar cells. *Journal of Physical Chemistry C*. 2012;**116**:10451-10460
- [8] Nattestad A et al. Highly efficient photocathodes for dye-sensitized tandem solar cells. *Nature Materials*. 2010;**9**:31-35
- [9] Yamaguchi T, Uchida Y, Agatsuma S, Arakawa H. Series-connected tandem dye-sensitized solar cell for improving efficiency to more than 10%. *Solar Energy Materials & Solar Cells*. 2009;**93**:733-736
- [10] Murayama M, Mori T. Dye-sensitized solar cell using novel tandem cell structure. *Journal of Physics D*. 2007;**40**:1664-1668
- [11] Kubo W, Sakamoto S, Kitamura T, Wada Y, Yanagida S. DSSC: Improvement of spectral response by tandem structure. *Journal of Photochemistry and Photobiology A*. 2004;**164**:33-39
- [12] Ito S et al. Optimization of the dye-sensitized solar cell with anthocyanin as photosensitizer. *Thin Solid Films*. 2008;**516**:4613-4619
- [13] Imahori H, Umeyama T, Ito S. Large π -aromatic molecules as potential sensitizers for highly efficient dye-sensitized solar cells. *Accounts of Chemical Research*. 2009;**42**:1809-1818
- [14] Bessho T, Zakeeruddin SM, Yeh CY, Diau EWG, Grätzel M. Highly efficient mesoscopic dye-sensitized solar cells based on donor-acceptor-substituted porphyrins. *Angewandte Chemie, International Edition*. 2010;**49**:6646-6649
- [15] Chien C-Y, Hsu B-D. Optimization of the dye-sensitized solar cell with anthocyanin as photosensitizer. *Solar Energy*. 2013;**98**:203-211
- [16] Cherepy NJ, Smestad GP, Grätzel M, Zhang JZ. Ultrafast electron injection: Implications for a photoelectrochemical cell utilizing an anthocyanin dye-sensitized TiO₂ nanocrystalline electrode. *The Journal of Physical Chemistry. B*. 1997;**101**:9342-9351
- [17] Aduloju KA, Shitta MB. Dye sensitized solar cell using natural dyes extracted from red leave onion.

International Journal of Physical Sciences. 2012;7:709-712

[18] Calogero G, Di Marco G. Red sicilian orange and purple eggplant fruits as natural sensitizers for dye-sensitized solar cells. *Solar Energy Materials and Solar Cells*. 2008;92:1341-1346

[19] Chang H, Lo YJ. Pomegranate leaves and mulberry fruit as natural sensitizers for dye-sensitized solar cells. *Solar Energy*. 2010;84:1833-1837

[20] Furukawa S, Iino H, Iwamoto T, Kukita K, Yamauchi S. Characteristics of dye sensitized solar cells using natural dye. *Thin Solid Films*. 2009;518:526-529

[21] Luo P, Niu H, Zheng G, Bai X, Zhang M, Wang W. From salmon pink to blue natural sensitizers for solar cells: *Canna indica* L., *salvia splendens*, cowberry and *Solanum nigrum* L. *Spectrochimica Acta Part A: Molecular and Biomolecular Spectroscopy*. 2009;74:936-942

[22] Calogero G, Yum JH, Sinopoli A, Di Marco G, Grätzel M, Nazeeruddin MK. Anthocyanins and betalains as light-harvesting pigments for dye-sensitized solar cells. *Solar Energy*. 2012;86:1563-1575

[23] Kumar K, Chowdhury A. Use of novel nanostructured photocatalysts for the environmental sustainability of wastewater treatments. In: Reference Module in Materials Science and Materials Engineering. Elsevier; 2018

[24] Grätzel M. Recent advances in sensitized mesoscopic solar cells. *Accounts of Chemical Research*. 2009;42(11):1788-1798

[25] Kamat PV, Das S, Thomas KG, George MV. Ultrafast photochemical events associated with the photosensitization properties of a squaraine dye. *Chemical Physics Letters*. 1991;178(1):75-79

[26] Kamat PV. Photoelectrochemistry in semiconductor particulate systems. 14. Picosecond charge-transfer events in the photosensitization of colloidal TiO₂. *Langmuir*. 1990;6(2):512-513

[27] Holkar CR, Jadhav AJ, Pinjari DV, Mahamuni NM, Pandit AB. A critical review on textile wastewater treatments: Possible approaches. *Journal of Environmental Management*. 2016;182:351-366

[28] Ge X, Timrov I, Binnie S, Biancardi A, Calzolari A, Baroni S. Accurate and inexpensive prediction of the color optical properties of anthocyanins in solution. *The Journal of Physical Chemistry. A*. 2015;119:3816. DOI: 10.1021/acs.jpca.5b01272

[29] Chemical Entities of Biological Interest (ChEBI). Online Molecular Database [Internet]. 2018. Available from: <https://www.ebi.ac.uk/chebi/> [Accessed: June 20, 2018]

[30] Woodford JN. A DFT investigation of anthocyanidins. *Chemical Physics Letters*. 2005;410:182

[31] Buseta PB, Colleter JC, Gadret M. Structure du chlorure d'apigéninidine monohydrate. *Acta Crystallographica. Section B*. 1974;30:1448

[32] Ueno K, Saito N. Cyanidin bromide monohydrate (3,5,7,3',4'-pentahydroxyflavylium bromide monohydrate). *Acta Crystallographica. Section B*. 1977;33:114

[33] Meyer M. Ab initio study of flavonoids. *International Journal of Quantum Chemistry*. 2000;76:724

[34] Skrede G, Wrolstad RE, Durst RW. Changes in anthocyanins and polyphenolics during juice processing of highbush blueberries (*Vaccinium*

- corymbosum* L.). Journal of Food Science. 2000;**65**:357-364
- [35] Veberic R, Jakopic J, Stampar F, Schmitzer V. European elderberry (*Sambucus nigra* L.) rich in sugars, organic acids, anthocyanins and selected polyphenols. Food Chemistry. 2009;**114**:511-515
- [36] Pedreschi R, Cisneros-Zevallos L. Phenolic profiles of andean purple corn (*Zea mays* L.). Food Chemistry. 2007;**100**:956-963
- [37] Dai Y, Rozema E, Verpoorte R, Choi YH. Application of natural deep eutectic solvents to the extraction of anthocyanins from *Catharanthus roseus* with high extractability and stability replacing conventional organic solvents. Journal of Chromatography. A. 2016;**1434**:50-56
- [38] Myjavcova R, Marhol P, Kren V, Simanek V, Ulrichova J, Palikova I, et al. Analysis of anthocyanin pigments in *Lonicera* (Caerulea) extracts using chromatographic fractionation followed by microcolumn liquid chromatography-mass spectrometry. Journal of Chromatography. A. 2010;**1217**:7932-7941
- [39] Maran JP, Priya B, Manikandan S. Modeling and optimization of supercritical fluid extraction of anthocyanin and phenolic compounds from *Syzygium cumini* fruit pulp. Journal of Food Science and Technology. 2014;**51**:1938-1946
- [40] Feuereisen MM, Gamero Barraza M, Zimmermann BF, Schieber A, Schulze-Kaysers N. Pressurized liquid extraction of anthocyanins and biflavonoids from *Schinus terebinthifolius* raddi: A multivariate optimization. Food Chemistry. 2017;**214**:564-571
- [41] Pap N, Beszédés S, Pongrácz E, Myllykoski L, Gábor M, Gyimes E, et al. Microwave-assisted extraction of anthocyanins from black currant marc. Food and Bioprocess Technology. 2012;**6**:2666-2674
- [42] Celli GB, Ghanem A, Brooks MS. Optimization of ultrasound-assisted extraction of anthocyanins from haskap berries (*Lonicera caerulea* L.) using response surface methodology. Ultrasonics Sonochemistry. 2015;**27**:449-455
- [43] Choi YH, Verpoorte R. Green solvents for the extraction of bioactive compounds from natural products using ionic liquids and deep eutectic solvents. Current Opinion in Food Science. 2019;**26**:87-93
- [44] Becke AD. Density-functional thermochemistry. III. The role of exact exchange. The Journal of Chemical Physics. 1993;**98**:5648
- [45] Frisch MJ et al. Gaussian 09, Revision D.01. Wallingford, CT: Gaussian, Inc; 2013
- [46] Terranova U, Bowler DR. Δ self-consistent field method for natural anthocyanidin dyes. Journal of Chemical Theory and Computation. 2013;**9**:3181
- [47] Fan W, Deng W. Incorporation of thiadiazole derivatives as π -spacer to construct efficient metal-free organic dye sensitizers for dye-sensitized solar cells: A theoretical study. Communications in Computational Chemistry. 2013;**1**:152
- [48] Armas R, Miguel M, Ovideo J, Sanz JF. Coumarin derivatives for dye sensitized solar cells: A TD-DFT study. Physical Chemistry Chemical Physics. 2012;**14**:225
- [49] Lopez JB, Gonzalez JC, Holguin NF, Sanchez JA, Mitnik DG. Density functional theory (DFT) study of triphenylamine-based dyes for their use as sensitizers in molecular photovoltaics.

International Journal of Molecular Sciences. 2012;**13**:4418

[50] Xu J, Zhang H, Liang G, Wang L, Xu W, Ciu W, et al. DFT studies on the electronic structures of indoline dyes for dye-sensitized solar cells. Journal of the Serbian Chemical Society. 2010;**75**:259

[51] Leonid S. Chemissian. V4. **43**:2005-2016

[52] Sanchez-Bojorge NA, Rodriguez-Valdez LM, Glossman-Mitnik MD, Flores-Holguin N. Theoretical calculation of the maximum absorption wavelength for cyanidin molecules with several methodologies. Computational and Theoretical Chemistry. 2015;**1067**:129

[53] Liu Z. Theoretical studies of natural pigments relevant to dye-sensitized solar cells. Journal of Molecular Structure: THEOCHEM. 2008;**862**:44

[54] Sanchez-de-Armas R, San-Miguel MA, Oviedo J, Sanz J. Direct vs. indirect mechanisms for electron injection in DSSC: Catechol and alizarin. Computational & Theoretical Chemistry. 2011;**975**:99

[55] Mitnik DG. Computational molecular characterization of coumarin-102. Journal of Molecular Structure: THEOCHEM. 2009;**911**:105

[56] Mohammadi N, Wang F. First-principles study of Carbz-PAHTDDT dye sensitizer and two carbz-derived dyes for dye sensitized solar cells. Journal of Molecular Modeling. 2014;**20**:2177

[57] Megala M, Rajkumar BJM. Theoretical study of anthoxanthin dyes for dye sensitized solar cells (DSSCs). Journal of Computational Electronics. 2016;**15**:557

[58] Harborne JB. Spectral methods of characterizing anthocyanins. The Biochemical Journal. 1958;**70**:22

[59] Brouillard R, Harborne JB, editors. The Flavonoids: Advances in Research Since 1980. London: Chapman and Hall Ltd; 1988. p. 525

[60] Harborne JB. Comparative Biochemistry of Flavonoids. London, New York: Academic Press; 1967